Desalination and Water Treatment
www.deswater.com
doi: 10.1080/19443994.2013.768446

51 (2013) 5231–5236
July

Taylor & Francis
Taylor & Francis Group

Preparation and characterization of amorphous carbon (a-C) membranes by molecular dynamics simulation

Mingming Zhai[a,b], Tomohisa Yoshioka[a,*], Jianhua Yang[b], Jinming Lu[b], Dehong Yin[b], Jinqu Wang[b,*]

[a]*Department of Chemical Engineering, Hiroshima University, Higashi-Hiroshima 739-8527, Japan*
Tel. +81 82 424 7719; Fax: +81 82 424 5494; email: tom@hiroshima-u.ac.jp
[b]*Faculty of Chemical, Environmental and Biological Science and Technology, Dalian University of Technology, Dalian 116-024, China*
Tel. +86 411 84986145; Fax: +86 411 84986149; email: wjinqu@dlut.edu.cn

Received 15 June 2012; Accepted 28 September 2012

ABSTRACT

Amorphous carbon (a-C) membranes with 1,728 particles were prepared from diamond at four different densities (1.8, 2.0, 2.28, and 2.4 g/cm^3) using molecular dynamics simulation. Stillinger and Weber potential for carbon was introduced with kinetic energy abided by classical Newton equation. Time mesh was chosen 0.01 or 1 fs. The melt-quenching technology method was adopted with the corresponding cooling rate 5 and 0.05 K/fs, respectively. Different membranes were obtained from higher initial temperature (7,500, 7,000, or 6,500 K at different densities and cooling rates) to room temperature. We compared the radial distribution function, bond angle distribution, and pore size distribution with experimental data. The results agreed well and one membrane at lower density with larger pores was chosen to calculate the gas permeation further. Gas molecules (He, Ne, H_2, CO_2, N_2, CH_4, and SF_6) permeation through the a-C membrane at low density (1.8 g/cm^3) when time mesh equal to 1 fs were calculated at 300, 400, 473, 500, and 600 K. The results of every gas species almost illustrated Knudsen diffusion well. And the number of permeated particles depended on the molecular weight.

Keywords: Amorphous carbon; Gas permeation; Molecular dynamics; Microscale pores

1. Introduction

Amorphous carbon (a-C) is a versatile material in the field of chemistry, optical, and electronic industry such as gas separation, wear-resistant coating, solar collector surfaces, magnetoresistance, field emission, etc. As far as we know, carbon constitutes different kinds of crystalline, graphite, or disordered structures because of the multiplicity of its hybridizations sp^1, sp^2, and sp^3 [1]. So a-Cs with various percentages of *sp*- hybridization have different densities [2]. In spite of last two decades of investigation on a-C, there still remain some debates over theoretical mechanism of a-C formation and properties. Molecular dynamics

*Corresponding authors.

7th Aseanian Membrane Society Conference (AMS7), 4–7 July 2012, Busan, Korea

Table 1
Parameters of SW potential [13] in this work

Parameter	Diamond
ε (eV)	3.214
σ (Å)	1.378
a	1.9
A	5.298
B	0.503
λ	24
γ	1.1
p; q	4; 0
$\cos\theta^{\circ}$	−1/3

(MD) simulation plays an important role in such further study. And it shows many advantages for a-C preparation by MD simulation. Since a generalized sp^2/sp^3 Stillinger and Weber (SW) potential [3] for carbon has been developed, the semi-empirical electronic potential was adopted on carbon atoms interaction, including 2-body bond stretching and 3-body bond bending.

After several different a-C configurations obtained, we have compared the major properties of a-C, such as radial distribution function (RDF), bond angle distribution (BAD), and pore size distribution (PSD). The performances of gas permeation are studied further by using MD simulation. The transport mechanism of small gas molecules through a-C structures, including large pores, should be analyzed which are usually classified as molecular sieving (configurational) diffusion, Knudsen diffusion, and surface diffusion [4–12].

2. Simulation method

In this work, the objectives are to prepare a-C membranes and to analyze gas permeation through them using MD method. MD represents one of the most effective methods to generate variety of micro- and macroscopic structures by solving motion equation. Since the melt temperature should be high

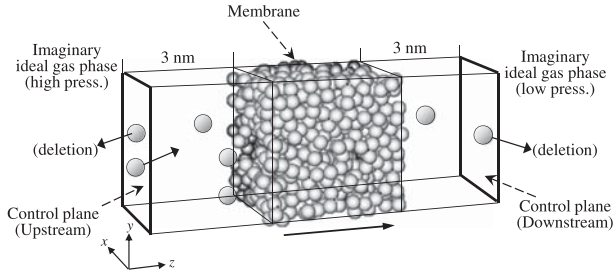

Fig. 1. Schematic image of a DCP-NEMD simulation cell.

enough to make sure the initial crystalline structure could be melt wholly, constant-NVT ensemble simulation and melt-quenching technology method from high temperature to room temperature was introduced, where N is the number of molecules, V is the volume and T is the temperature. The calculation time has relationship with time mesh. Since a generalized sp^2/sp^3 semi-empirical electronic SW potential $\Phi(2,3)$ [3] for carbon has been developed, it was adopted on carbon atoms interaction, including two-body bond stretching $\upsilon_{ij}^{(2)}(r_{ij})$ and three-body bond bending $\upsilon_{jik}^{(3)}(\mathbf{r}_{ij},\mathbf{r}_{ik})$. The SW potential was described by Eqs. (1)–(3) as follows.

$$\Phi(2,3) = \varepsilon\left[\sum_{\langle ij\rangle}\upsilon_{ij}^{(2)}(r_{ij}) + \sum_{\langle jik\rangle}\upsilon_{jik}^{(3)}(r_{ij},r_{ik})\right] \tag{1}$$

$$\upsilon_{ij}^{(2)}(r_{ij}) = A\left[B(r_{ij}/\sigma)^{-p} - (r_{ij}/\sigma)^{-q}\right]\exp(r_{ij}/\sigma - a)^{-1} \tag{2}$$

$$\upsilon_{jik}^{(3)}(\mathbf{r}_{ij},\mathbf{r}_{ik}) = \lambda\left[\exp(\gamma(r_{ij}/\sigma - a)^{-1}) + \exp(\gamma(r_{ik}/\sigma - a)^{-1})\right] \times (\cos\theta_{jik} - \cos\theta^{0})^2 \tag{3}$$

where ε and σ are energy and length units, respectively, r_{ij}, r_{ik} the inter-particle separation distance; A, B, λ, and γ the parameters of the short range repulsive term; a the cutoff distance; θ_{jik} the angle between r_j and r_k subtended at vertex i; θ^0 the ideal tetrahedral angle in diamond-like structures. The parameter values are listed in Table 1.

Table 2
LJ parameters of different gases in this simulation

Gas species	C [14]	He [15]	Ne [15]	H_2 [15]	CO_2 [15]	N_2 [16]	CH_4 [16]	SF_6 [17]
w (g/mol)	12.01	4.00	20.18	2.02	44.01	28.01	16.04	146.06
ε_i/k_B (K)	28.02	10.22	35.0	38.0	195.2	72.89	148.0	201
σ_i (Å)	3.37	2.60	2.78	2.90	3.30	3.64	3.73	5.51

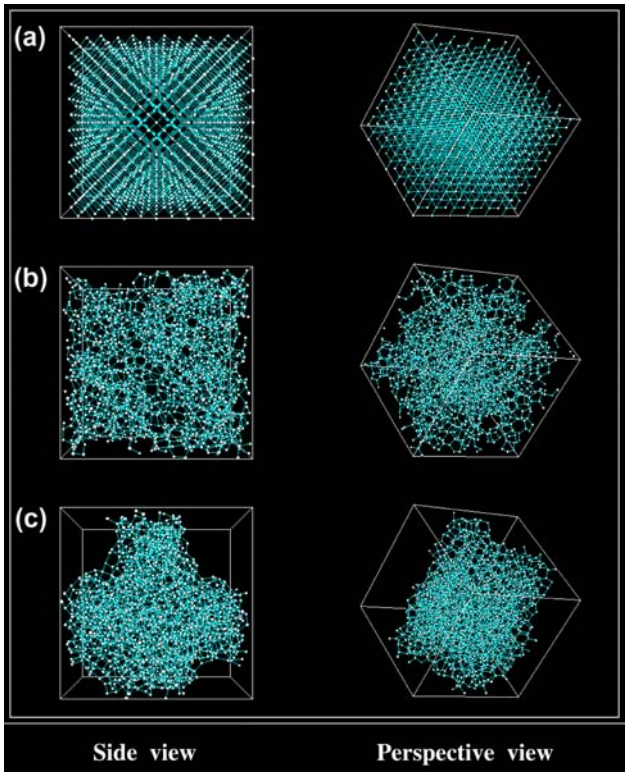

Fig. 2. Snapshots of (a) crystalline and; (b) a-C at 1.8 g/cm^3, time mesh 0.01 fs; (c) a-C at1.8 g/cm^3, time mesh 1 fs, on side (x-y plane) and perspective view, respectively, calculated by MD simulation.

For interactions between permeating gas molecules and carbon atoms, and among gas molecules, the widely known Lennard-Jones (LJ) potential is given by Eq. (4).

$$E(r_{ij}) = 4\varepsilon_{ij}\left[\left(\frac{\sigma_{ij}}{r_{ij}}\right)^{12} - \left(\frac{\sigma_{ij}}{r_{ij}}\right)^{6}\right] \quad (4)$$

The relative potential parameters are illustrated by Table 2.

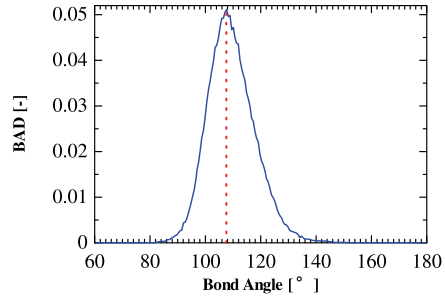

Fig. 4. BAD, $\rho = 1.8\,g/cm^3$, time mesh = 1 fs.

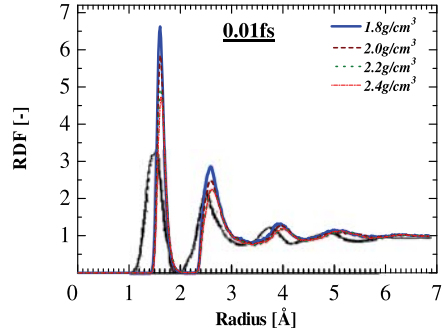

Fig. 5. RDF, time mesh = 0.01 fs.

The main research of this work consists of two steps, a-Cs preparation and gas permeation.

Firstly, we used the SW parameters due to Gerstner et al. [13] to generate a-Cs with periodic boundary conditions. The number of carbon atoms was 1,728 to ensure certain a thickness of membranes. Densities depended on the range of real situation. Time mesh had much effect on the homogenization, so 1 and 0.01 fs were set. The cooling rate of melt-quenching method was selected 5 K/100 step. Melt temperatures were 6,500, 6,500, 7,000, and 7,500 K for the density equal to 1.8, 2.0, 2.2, and 2.4 g/cm^3, respectively.

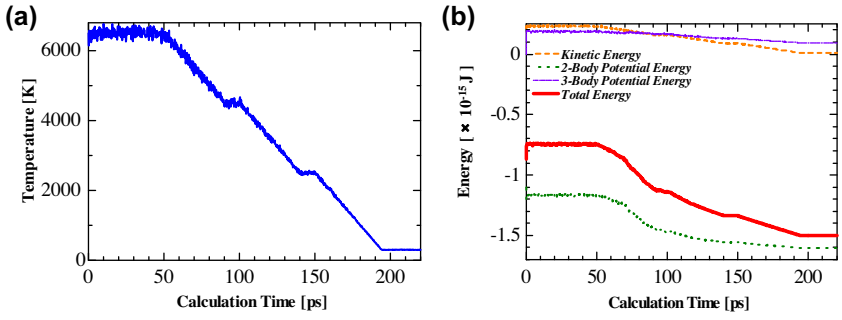

Fig. 3. Temperature control (a) and energy change (b) on calculation time, $\rho = 1.8\,g/cm^3$, time mesh = 1 fs.

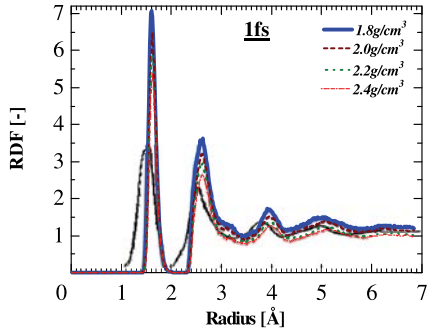

Fig. 6. RDF, time mesh = 1 fs.

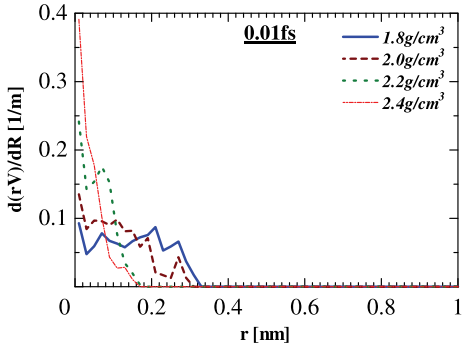

Fig. 7. PSD, time mesh = 0.01 fs.

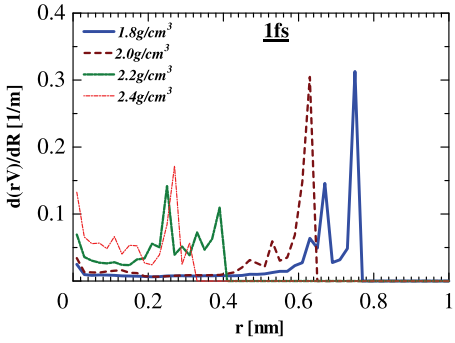

Fig. 8. PSD, time mesh = 1 fs.

After the a-C membranes were gotten, temperature variation, two-body, three-body, kinetic, and total energy in the whole process were all calculated. By the results of the temperature and total energy, we were able to choose the stable calculation time of a-C structures at room temperature. To observe the characteristics of those structures, BAD, RDF, and PSD were calculated sequentially. Therefore, the most reasonable membrane was selected to calculate the gas permeation next.

Secondly, the significant demand for gas permeation simulation was that permeation properties should be provided at the steady state. As a result,

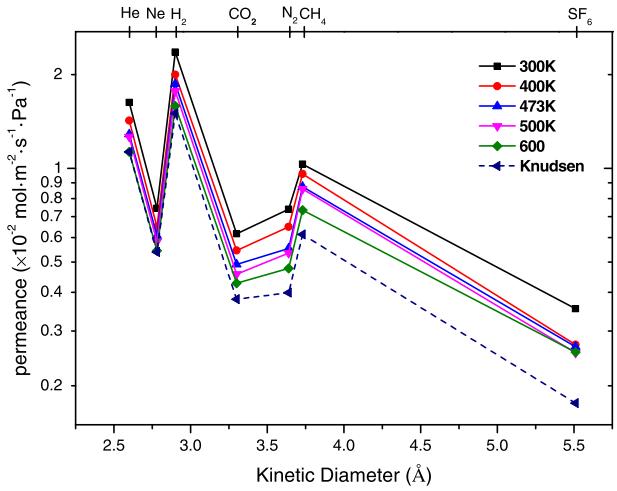

Fig. 9. Kinetic diameters dependency of gas permeance through a-C. $\rho = 1.8\ g/cm^3$, time mesh = 1 fs.

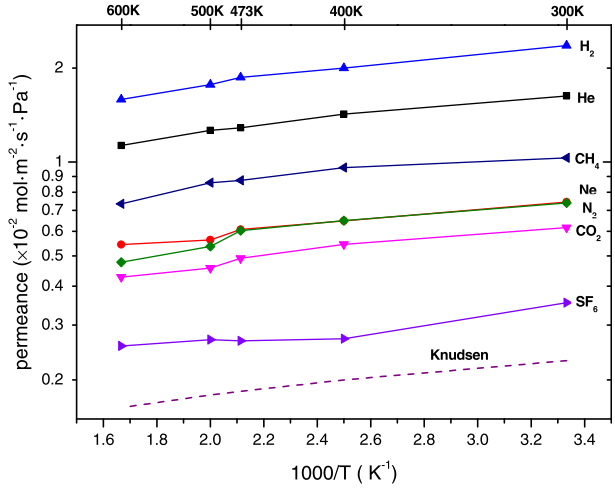

Fig. 10. Temperature dependency of gas permeance through a-C, $\rho = 1.8\ g/cm^3$, time mesh = 1 fs.

the boundary plane with an imaginary gas phase was needed on which the permeating gas particles could be produced or deleted [18,19]. The idea allowed a changeable number of permeating particles so as to keep the system steady and reasonable. It was an ingenious setting to attain the steady state with the given upstream and downstream pressure. Fig. 1 shows a schematic image of the unite cell by dual control plane non-equilibrium (DCP-NEMD) method used in our simulation. Gas molecules permeated through the membrane in the z-direction from the higher pressure side to the lower pressure side. Permeating molecules were introduced from the boundary plane in the frequency, f, by Eq. (5), which is corresponded to the value under the specified temperature and pressure.

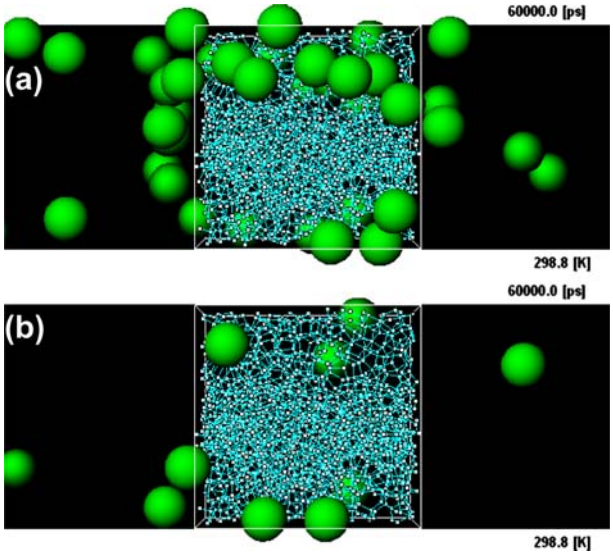

Fig. 11. Snapshots of SF_6 permeation. (a) 300 K and (b) 500 K, at 1.8 g/cm^3, time mesh 1 fs.

$$\text{frequency} = \frac{pS}{\sqrt{2\pi mkT}} \tag{5}$$

where p is gas phase pressure; S is the area of the boundary plane, T the temperature.

3. Results and discussion

Firstly, a-C (Fig. 2(b) and (c)) membranes were gotten from crystalline structures (Fig. 2(a)) at different densities and time mesh. From Fig. 2(a), the unit cell of diamond could be seen clearly. Each smallest cell contains 8 carbon molecules, every particle had three single bonds and the bond angle was 109.5°. It was the reason why $\cos\theta^\circ$ was equal to $-1/3$ ideally. The side view was on the direction of x-y plane. Fig. 2(b) represented a-C membrane at 1.8 g/cm^3, 0.01 fs, and Fig. 2(c) at 1.8 g/cm^3, 1 fs.

Fig. 3(a) depicted temperature control with calculation time, while Fig. 3(b) energy change, when $\rho = 1.8$ g/cm^3, time mesh = 1 fs. For Fig. 3(a), at the first step about 50 ps, the diamond melted to be amorphousness, then quenching down by several steps to room temperature. At the last step, a-C kept stable on both temperature and energies. Hence from around 200 ps to the end, the next calculation could be done in reasonable situation.

BAD showed obvious amorphousness in Fig. 4. RDFs at different densities were compared with experimental reported data by Alvarez et al. [20]. The RDF data in Figs. 5 and 6 illustrated amorphous state because there almost were no apparent peaks at lager distance than the second peak located. It showed an interesting behavior as Alvarez' *ab initio* simulation: the peaks are slightly displaced toward the larger side of the interatomic distances. This indicated the presence of sp^2 bonds.

Figs. 7 and 8 displayed that different time mesh generated different amorphous structures, which also could be verified by the snapshots (see Fig. 2). They illustrated that shorter time mesh resulted in more uniform structures, and these homogeneous membranes were too dense to make even small gas molecules permeate through them. On the other hand, Fig. 8 showed that longer time mesh could lead to some large pores. So we preferred that membrane, that is at the density of 1.8 g/cm^3, time mesh equal to 1 fs, for further study on gas permeation.

Fig. 9 displayed kinetic diameters dependency of permeance. We could find that the permeance was depended not only on the size of gas molecules but also on the molecular weight. Fig. 10 was consistent with the conclusion in another way. It is the temperature dependency of gas permeance. Helium permeation was almost as same as the simple Knudsen curve given by Eq. (6) [21].

$$P_k = \frac{k_g}{\sqrt{MRT}} \tag{6}$$

where k_g is a geometrical factor depending on the pore structure. Comparing with it, gas molecules had almost the same dependency which belonged to Knudsen diffusion except sulfur hexafluoride. The bigger size gas molecules SF_6 at higher temperature above 400 K followed slightly activated diffusion, while at lower temperature, it abided by surface diffusion since the slope of its permeance line was a little larger.

As shown in the snapshots of sulfur hexafluoride molecules permeation at two different temperatures (a) 300 K and (b) 500 K in Fig. 11, SF_6 molecules also followed active diffusion at higher temperature; and it turned to surface diffusion when the temperature was lower. Because when temperature was higher, activation energy made more effect. Experimental study on the preparation of membranes and prediction of their separation factor has been reported elsewhere [22].

4. Conclusion

Amorphous carbon (a-C) membranes at different densities could be successfully obtained by our MD simulation. Time mesh was a very important factor to generate different structures at the same density. The smaller time mesh was set, the more homogeneous

membrane was obtained, while a little more running time was taken. Melt-quenching technology is feasible and valid method to get a structure by our MD simulation. Energies of the system showed reasonable behavior by the SW two-body and three-body potentials to reach a steady state. From BAD, RDF, and PSD, we could observe good agreement with experiment and other simulation results. In this work, when time mesh was equal to 1 fs, density 1.8 g/cm^3 could be obtained. The a-C membrane was selected to study further gas permeation. On the other hand, an inhomogeneous a-C model with larger pores could be obtained. It showed better homogeneity when time mesh was set 0.01 fs.

DCP-NEMD method provided an advantageous project to simulate gas permeation properties. Different gas species molecules permeation showed almost the Knudsen diffusion properties. And the number of permeated particles was depended on the weight of gas molecules, and the order was $H_2 > He > CH_4 > Ne > N_2 > CO_2 > SF_6$.

Acknowledgments

Thanks to China Scholarship Council (CSC) for financial support for overseas students when the author works in Japan. Especially, the author was grateful to Prof. Yoshioka, Prof. Tsuru, and Prof. Kanezashi for their great help in our study, not only to the research support and guidance but also to provide many a chance to make so much progress. And the author would like to thank prof. Wang and Prof. Yang in Dalian University of Technology to provide their great help.

References

[1] J. Roberton, Diamond-like amorphous carbon, Mater. Sci. Eng. R 37 (2002) 129–281.
[2] A.C. Ferrari, A. Libassi, B.K. Tanner, V. Stolojan, J. Yuan, L. M. Brown, S.E. Rodil, B. Kleinsorge, J. Robertson, Density, sp^3 fraction, and cross-sectional structure of amorphous carbon films determined by x-ray reflectivity and electron energy-loss spectroscopy, Phys. Rev. B 62 (2000) 11089–11103.
[3] F.H. Stillinger, T.A. Weber, Computer simulation of local order in condensed phases of silicon, Phys. Rev. B 31 (1985) 5262–5271.
[4] A.B. Shelekhin, A.G. Dixon, Y.H. Ma, Theory of gas diffusion and permeation in inorganic molecular-sieve membranes, AIChE J. 41 (1995) 58–67.
[5] A.J. Burggraaf, Single gas permeation of thin zeolite (MFI) membranes: Theory and analysis of experimental observations, J. Membr. Sci. 155 (1999) 45–65.
[6] T. Yoshioka, T. Tsuru, M. Asaeda, Condensable vapor permeation through microporous silica membranes studied with molecular dynamics simulation, Sep. Purif. Technol. 32 (2003) 231–237.
[7] F.N. Tüzün, E. Arçevik, Pore modification in porous ceramic membranes with sol-gel process and determination of gas permeability and selectivity, Macromol. Symp. 287 (2010) 135–142.
[8] A.P. Soldatov, G.N. Evtyugina, D.A. Syrtsova, O.P. Parenago, A new method of modification of inorganic membranes with pyrocarbon nano-sized crystallites, Russ. J. Phys. Chem. A 84 (2010) 648–655.
[9] P.F. Lito, C.F. Zhou, A.S. Santiago, A.E. Rodrigues, J. Rocha, Z. Lin, C.M. Silva, Modelling gas permeation through new microporous titanosilicate AM-3 membranes, Chem. Eng. J. 165 (2010) 395–404.
[10] M. Ostwal, R.P. Singh, S.F. Dec, M.T. Lusk, J.D. Way, 3-Aminopropyltriethoxysilane functionalized inorganic membranes for high temperature CO_2/N_2 separation, J. Membr. Sci. 369 (2011) 139–147.
[11] S.K. Wirawan, D. Creaser, J. Lindmark, J. Hedlund, I.M. Bendiyasa, W.B. Sediawan, H_2/CO_2 permeation through a silicalite-1 composite membrane, J. Membr. Sci. 375 (2011) 313–322.
[12] L. Ge, L. Wang, A. Du, M. Hou, V. Rudolph, Z. Zhu, Vertically-aligned carbon nanotube membranes for hydrogen separation, RCS Adv. 12 (2012) 5329–5336.
[13] E.G. Gerstner, B.A. Pailthorpe, Molecular dynamics simulation of thin film amorphous carbon growth, J. Non-Cryst. Sol. 189 (1995) 258–264.
[14] S. Sokolowski, W. Steele, Molecular dynamics studies of argon-diluted nitrogen films adsorbed on graphite, Mol. Phys. 54 (1985) 1453–1468.
[15] T. Yoshioka, T. Tsuru, M. Asaeda, Molecular dynamics study of gas permeation through amorphous silica network and inter-particle pores on microporous silica membranes, Mol. Phys. 102 (2004) 191–202.
[16] S.J. Mahdizadeh, S.F. Tayyari, Methane storage in homogeneous armchair open-ended single-walled boron nitride nanotube triangular arrays: a grand canonical Monte Carlo simulation study, J Mol. Model 18 (2012) 2699–2708.
[17] A.M. Mainar, J. Pardo, J.I. García, F.M. Royo, J.S. Urieta, Solubility of gases in fluoroorganic alcohols: Part I. Solubilities of several non-polar gases in 1,1,1,3,3,3-hexafluoropropan-2-ol at 298.15 K and 101.33 kPa, J. Chem. Soc., Faraday Trans., 94 (1998) 3595–3599.
[18] M. Miyahara, T. Yoshioka, J.I. Nakamura, M. Okazaki, Simple evaluation scheme of adsorbate-solid interaction for nanopore characterization studied with Monte Carlo simulation, J. Chem. Eng. Jpn. 33 (2000) 103–112.
[19] T. Yoshioka, M. Asaeda, T. Tsuru, A molecular dynamics simulation of pressure-driven gas permeation in a micropore potential field on silica membranes, J. Membr. Sci. 293 (2007) 81–93.
[20] F. Alvarez, C.C. Díaz, R.M. Valladares, A.A. Valladares, Ab initio generation of amorphous carbon structures, Diamond Relat. Mater. 11 (2002) 1015–1018.
[21] T. Yoshioka, A. Yasumoto, K. Kishi, T. Tsuru, MD simulation studies for effect of membrane structures and dynamics on gas permeation properties through microporous amorphous silica membranes, Desalination 233 (2008) 333–341.
[22] J. Wang, T. Yoshioka, M. Kanezashi, T. Tsuru, Prediction of pervaporation performance using aqueous ethanol solutions based on single gas permeation, Desal. Water Treat. 17 (2010) 106–111.